




Article

Enhancing the Hardness and Compressive Response of Magnesium Using Complex Composition Alloy Reinforcement

Khin Sandar Tun ¹ , Yuming Zhang ², Gururaj Parande ¹ , Vyasraj Manakari ¹  and Manoj Gupta ^{1,*}

¹ Department of Mechanical Engineering, National University of Singapore, Singapore 117576, Singapore; mpekst@nus.edu.sg (K.S.T.); gururaj.parande@u.nus.edu (G.P.); mbvyasaraj@u.nus.edu (V.M.)

² Department of Mechanical & Industrial Engineering, University of Toronto St. George Campus, Toronto, ON M5S 1A1, Canada; yuming.zhang@mail.utoronto.ca

* Correspondence: mpegm@nus.edu.sg; Tel.: +65-6516-6358

Received: 22 March 2018; Accepted: 14 April 2018; Published: 17 April 2018



Abstract: The present study reports the development of new magnesium composites containing complex composition alloy (CCA) particles. Materials were synthesized using a powder metallurgy route incorporating hybrid microwave sintering and hot extrusion. The presence and variation in the amount of ball-milled CCA particles (2.5 wt %, 5 wt %, and 7.5 wt %) in a magnesium matrix and their effect on the microstructure and mechanical properties of Mg-CCA composites were investigated. The use of CCA particle reinforcement effectively led to a significant matrix grain refinement. Uniformly distributed CCA particles were observed in the microstructure of the composites. The refined microstructure coupled with the intrinsically high hardness of CCA particles (406 HV) contributed to the superior mechanical properties of the Mg-CCA composites. A microhardness of 80 HV was achieved in a Mg-7.5HEA (high entropy alloy) composite, which is 1.7 times higher than that of pure Mg. A significant improvement in compressive yield strength (63%) and ultimate compressive strength (79%) in the Mg-7.5CCA composite was achieved when compared to that of pure Mg while maintaining the same ductility level. When compared to ball-milled amorphous particle-reinforced and ceramic-particle-reinforced Mg composites, higher yield and compressive strengths in Mg-CCA composites were achieved at a similar ductility level.

Keywords: magnesium; high entropy alloy; composite; hardness; compressive properties

1. Introduction

Magnesium (Mg) is the lightest of all structural metals and possesses the highest strength-to-density ratio. In addition, magnesium has other favorable advantages, including a high damping capacity, high dimensional stability, good machinability, good electromagnetic shielding characteristics, and recyclability. Accordingly, magnesium is the designers' choice for possible production of lightweight vehicles to meet the demand of reducing greenhouse emissions [1–3]. Magnesium is mostly used in the form of alloys in commercial applications [4,5]. With the advent of composite technology, research interest has been placed on the development of high-performance magnesium composites. By a careful selection of matrix and reinforcing phases, newly formed composite materials with significant improvements in elastic modulus, strength, ductility, and coefficient of thermal expansion can be fabricated. Composite materials are attractive because they offer the possibility for combining useful engineering properties of individual elements, which is otherwise not possible from monolithic materials. The attractive physical and mechanical properties obtained from metal

matrix composites (MMCs) have made them potential candidates for aerospace, automotive, and other structural applications [6]. For the fabrication of magnesium composites, various types of ceramic reinforcements, such as alumina (Al_2O_3), yttria (Y_2O_3), zirconia (ZrO_2), silicon carbide (SiC), boron carbide (B_4C), and titanium carbide (TiC), have been used in Mg matrix [7–11]. In addition to ceramic reinforcements, research efforts have been made to synthesize Mg composites using metal particle reinforcements, such as copper, nickel, titanium, molybdenum, and aluminum [11,12]. Investigations have also been made on Mg composites containing hybrid reinforcements in the form of ceramic plus metal, ceramic plus ceramic, and ceramic plus carbon nanotube (CNT) besides single ceramic, metal, and CNT reinforcements [11,13–16]. In a recent development on magnesium composites, ball-milled amorphous particles were also used as a reinforcement in a pure magnesium matrix [17–19].

In the present study, an attempt is made to develop new magnesium composites using ball-milled complex composition alloy (CCA) particles. From the thermodynamic calculation, the current complex composition alloy has a high entropy value (ΔS_{mix}) of 12.97 J/K mol. Based on the concept of configurational entropy, the multicomponent alloys having a mixing or configurational entropy value which is equivalent to or greater than 12.471 J/K mol ($\Delta S_{\text{conf}} \geq 1.5R$ (12.471), where R is the gas constant), are regarded as high entropy alloys (HEAs). According to this concept, the CCA used in this study can be classified under the category of high entropy alloys. A careful examination of the published literature reveals that no attempt has been made to investigate the microstructure and mechanical properties of magnesium using ball-milled CCA particles. A powder metallurgy route incorporating microwave-assisted rapid sintering coupled with hot extrusion was used to synthesize Mg and Mg-CCA composites. The effect of the presence of CCA particles on microstructure and mechanical properties of magnesium was investigated. The interrelation between microstructure and mechanical properties of Mg-CCA composites was studied. The properties of Mg-CCA composites when varying the amount of reinforcement alloy particles are reported and the test results are benchmarked against pure magnesium.

2. Materials and Methods

2.1. Synthesis of Materials

In this study, magnesium powder of 98.5% purity and with a size range of 60–300 μm (Merck, Darmstadt, Germany) was used as the matrix material. Ball-milled CCA particles were used as the particulate reinforcements. Initially, CCA pieces from cast ingot with composition $\text{Al}_{35}\text{Mg}_{30}\text{Si}_{13}\text{Zn}_{10}\text{Y}_7\text{Ca}_5$ [20] were crushed into particles by ball milling the cast pieces at 200 rpm for 30 minutes with a ball to cast pieces weight ratio of 10:1 in a RETSCH PM-400 mechanical alloying machine (RETSCH, Haan, Germany). Monolithic magnesium and magnesium composites (Mg-2.5 wt % CCA, Mg-5 wt % CCA, and Mg-7.5 wt % CCA) were synthesized using a powder metallurgy technique. The synthesis process for Mg-CCA composites involved blending pure magnesium powder with CCA particles using the same machine at 200 rpm for 1 h without the use of grinding balls. The blended powder mixtures were then cold compacted using a 100-ton press to form billets that measured 35 mm in diameter and 45 mm in height. Monolithic magnesium was compacted using the same parameters without blending. The compacted billets were then sintered using a hybrid microwave sintering technique for 16 min to reach a temperature of 640 °C near the melting point of magnesium using a 900 W, 2.45 GHz SHARP microwave oven (Sharp Corporation, Osaka, Japan). The sintered billets were homogenized at 400 °C for 1 h and subsequently hot extruded at a temperature of 350 °C at an extrusion ratio of 20.25:1.

2.2. Characterization

Microstructural characterization studies were conducted on the extruded polished samples to determine the grain size, grain morphology, and presence and distribution of reinforcements. An Olympus metallographic optical microscope (Olympus Corporation, Shinjuku, Tokyo, Japan),

MATLAB analysis software (R2013b, MathWorks, Natick, MA, USA), and a JEOL JSM-6010 scanning electron microscope (JEOL Ltd., Tokyo, Japan) were used for this purpose. X-ray diffraction analysis was conducted using an automated Shimadzu LAB-XRD-6000 (Shimadzu Corporation, Kyoto, Japan) (Cu K α : $\lambda = 1.54056 \text{ \AA}$) spectrometer with a scan speed of 2 degrees per minute.

Microhardness measurements were performed on the polished samples using a Shimadzu-HMV automatic digital microhardness tester (Shimadzu Corporation, Kyoto, Japan) with a Vickers indenter. An indentation load of 245.5 mN and a dwell time of 15 s was used in accordance with the ASTM standard E384-08.

Room temperature compression tests were performed on cylindrical monolithic and composite samples according to ASTM E9-89a using an automated servo hydraulic testing machine MTS810 (MTS systems corporation, Eden Prairie, MN, USA). An extruded rod 8 mm in diameter was cut into 8 mm-long samples for compression tests to provide the aspect ratio (length/diameter) of unity. Samples were tested at a strain rate of $5 \times 10^{-3} \text{ min}^{-1}$ and the compression load was applied parallel to the extrusion direction.

Fracture surface characterization studies were carried out on the compressively fractured surfaces of Mg and Mg composites with the objective of establishing the failure mechanisms. Fractography was accomplished using a JEOL JSM-6010 scanning electron microscope (SEM).

3. Results and Discussion

3.1. Analysis on Reinforcement Particles

Figure 1a shows the size and morphology of the ball-milled CCA particles. The average particle size was calculated to be $2.7 \pm 1.4 \text{ }\mu\text{m}$. The morphology of the particles can be seen as irregular shape although the smallest particles were almost spherical. The particle distribution can be seen in Figure 1b, and the particle sizes ranged from 1 μm to 7 μm with the dominant particle size in the range of 2–3 μm . The measured bulk microhardness of the cast materials was found to be very high at $406 \pm 15 \text{ HV}$ ($4 \pm 0.1 \text{ GPa}$) [20]. The XRD profiles of cast CCA and ball-milled CCA particles can be seen in Figure 2. The main phases found in the cast materials were maintained in the ball-milled version of the CCA material. The prominent change in the XRD pattern of ball-milled CCA particles is the broadening of the peaks, which may be attributed to the transformation of particles from the bulk material and an increase in the solid solubility of elements (Figure 2).

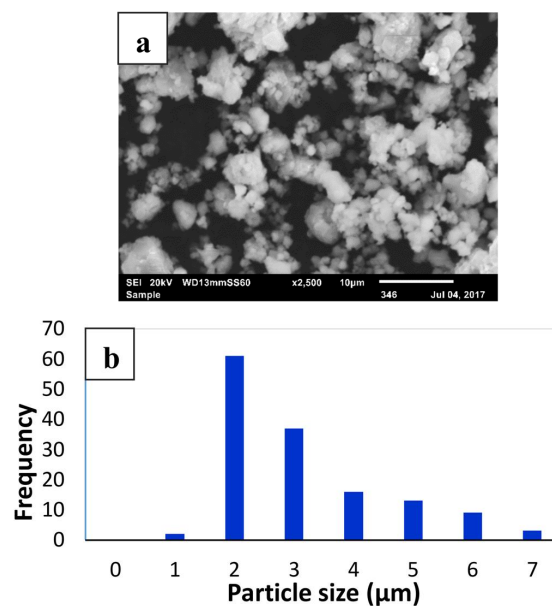


Figure 1. S scanning electron microscope (SEM) micrograph showing the morphology of ball-milled complex composition alloy (CCA) particles in (a) and the graph showing particle distribution in (b).

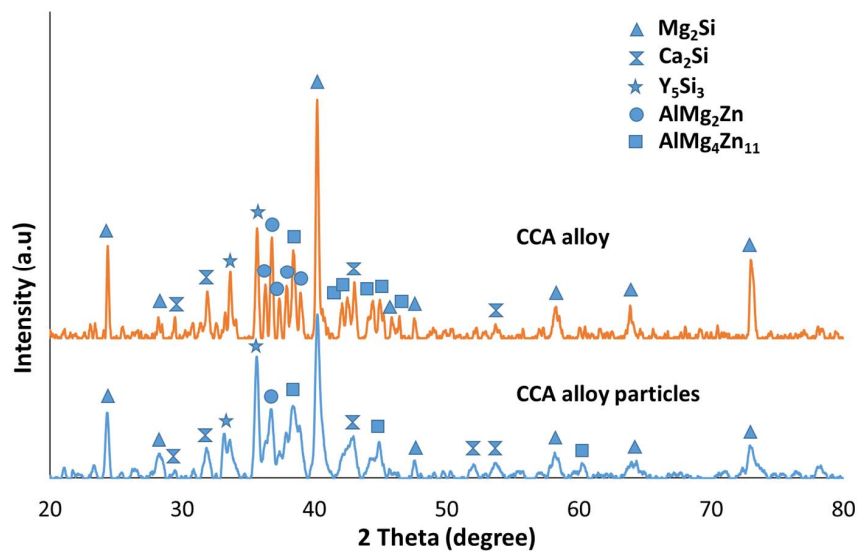


Figure 2. X-ray diffraction (XRD) pattern of the cast CCA alloy and ball-milled CCA alloy particles.

3.2. Microstructure

The distribution pattern of CCA reinforcement particles in the Mg matrix is shown in Figure 3b–d. For comparison purpose, the SEM micrograph of Mg is shown in Figure 3a. With the addition of 2.5 wt % CCA particles, the presence of uniformly distributed reinforcement particles can be seen in the micrograph (Figure 3b). In Mg-5CCA's composition, the reinforcement particles were reasonably distributed in the Mg matrix (Figure 3c). However, with the increased addition of CCA particles from 2.5 wt % to 5 wt %, the tendency for the formation of particle clustering can be seen in the micrograph and the particles were mostly decorated at the particle/grain boundaries (Figure 3c). In the case of Mg-7.5CCA's composition, in spite of having an increased amount of HEA particles, the HEA particles were uniformly distributed with limited evidence of particle clustering (Figure 3d) in the Mg matrix.

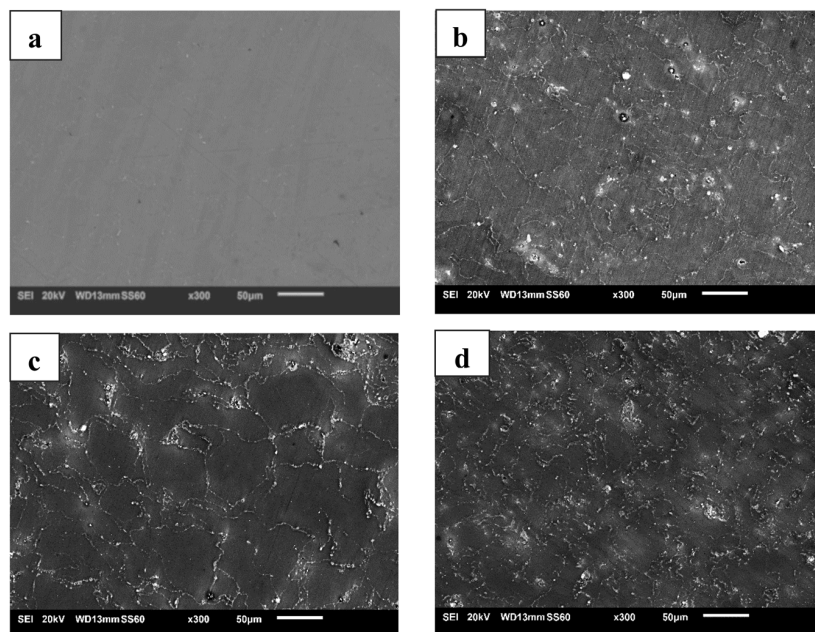


Figure 3. SEM micrographs of the: (a) Mg and CCA particle distribution in the (b) Mg-2.5CCA; (c) Mg-5CCA; and (d) Mg-7.5CCA composites.

The grain size and grain morphology of Mg and Mg-CCA composites are shown in Table 1 and Figure 5. The grain morphology was found to be nearly equiaxed and the grain size decreased with increasing presence of reinforcement particles up to 5 wt %. Further increase in the amount of particles from 5 wt % to 7.5 wt % had no effect on grain size reduction and the average grain size remained the same in both the Mg-5CCA and Mg-7.5CCA composites. However, from the grain size distribution analysis, the grain size distribution was more homogeneous in Mg-7.5CCA's composition (Figure 4d) when compared to Mg-5CCA's composition (Figure 4c). While having the same average grain size in both compositions, the presence of small-sized grains was found to be more frequent in Mg-5CCA's composition when compared to Mg-7.5CCA's composition. In fact, the distribution graph resembles a right-skewed distribution in Mg-5CCA's composition while a normal distribution pattern was observed in the Mg, Mg-2.5CCA, and Mg-7.5CCA composites.

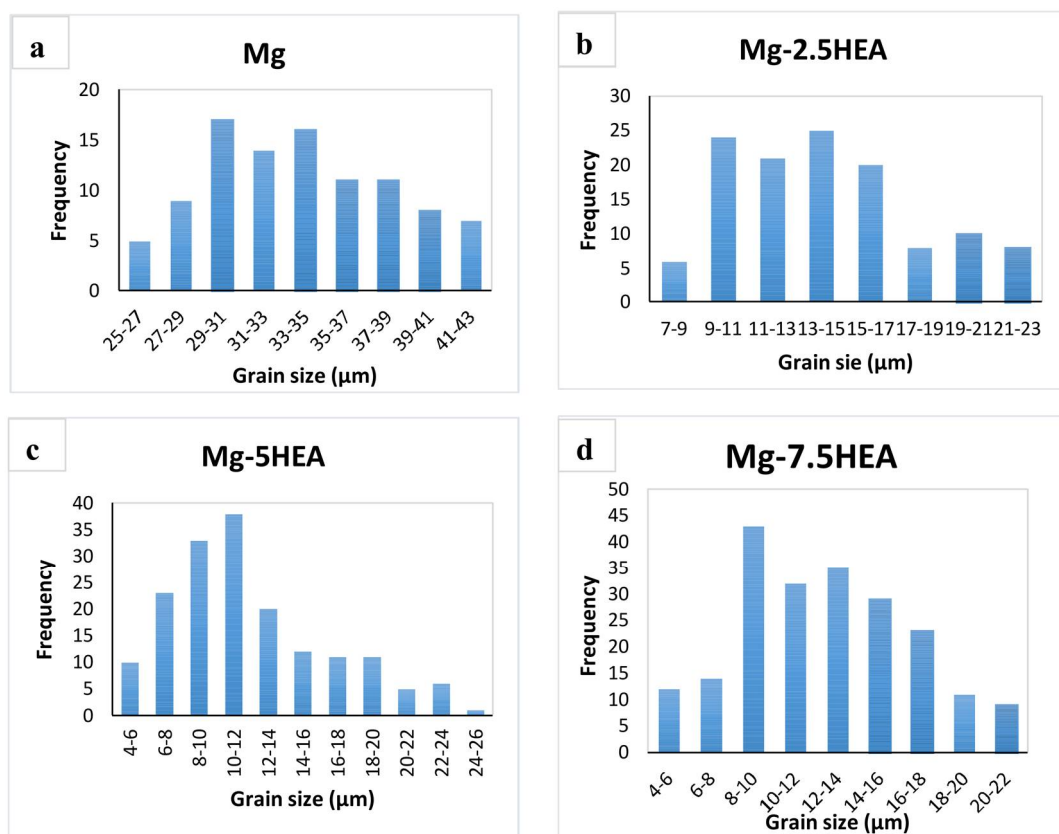


Figure 4. Grain size distribution graphs of the: (a) Mg and (b) Mg-2.5CCA; (c) Mg-5CCA; and (d) Mg-7.5CCA composites.

Table 1. Results of grain morphology and microhardness.

Materials	Grain Size (μm)	Aspect Ratio	Microhardness (HV)
Mg	34 ± 4	1.4 ± 0.3	47 ± 2
Mg-2.5 wt % CCA	14 ± 4	1.4 ± 0.3	56 ± 6
Mg-5.0 wt % CCA	12 ± 5	1.5 ± 0.3	70 ± 6
Mg-7.5 wt % CCA	12 ± 4	1.5 ± 0.3	80 ± 7

Since the reinforcement particle size used for the synthesis of Mg composites was at the micron length scale, particle-stimulated dynamic recrystallization during hot extrusion can be expected [21,22]. The more evenly distributed grain size (Figure 5) in the case of Mg-7.5CCA versus Mg-5HEA can be attributed to a more uniform distribution and a larger number of CCA particles in the former [23].

In extruded Mg composites, the recrystallized grains have common boundaries with the particles. With the more homogeneous distribution of particles throughout the matrix coupled with the increased presence of particles, it is possible that the migration of grain boundaries was prevented by the particles and hence the grain growth. This will provide more evenly distributed grains in the Mg-7.5CCA composite and hence while the largest grains observed in the Mg-5CCA composite measured in the range of 24–26 μm , it was only 20–22 μm in the case of the Mg-7.5CCA composite.

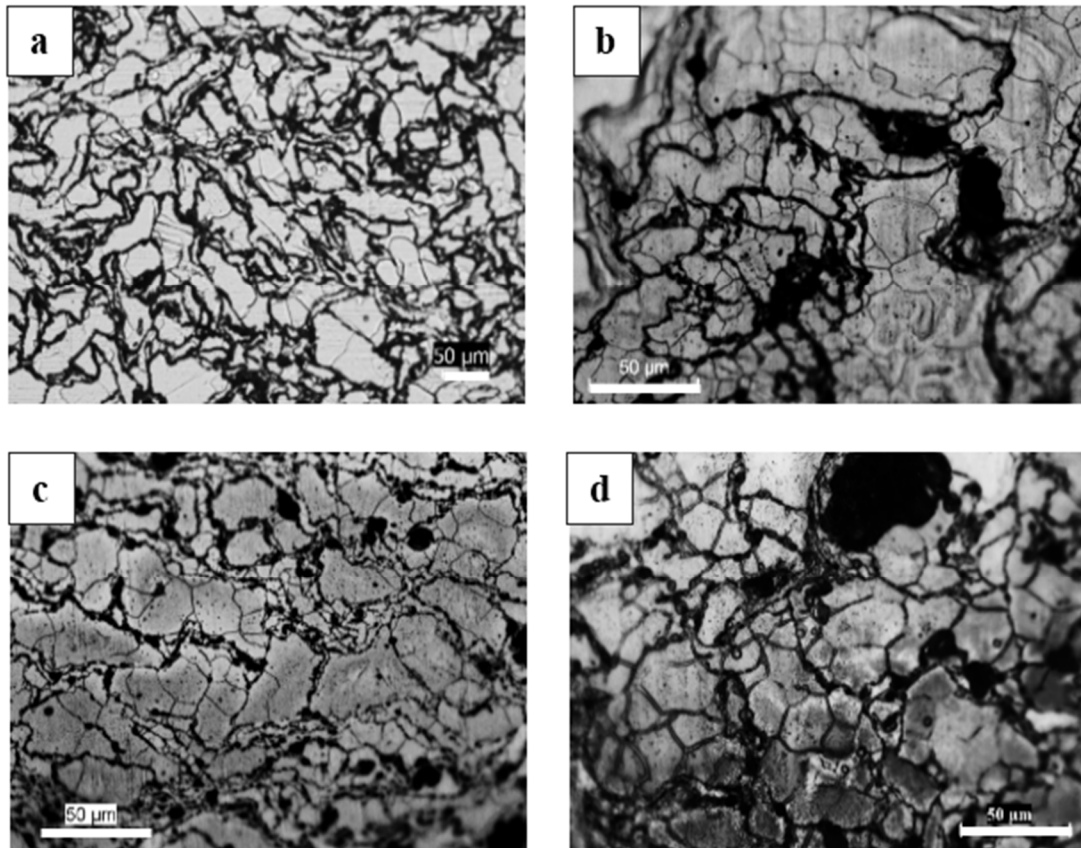


Figure 5. The grain size distribution pattern in the etched surfaces of the: (a) Mg; (b) Mg-2.5CCA; (c) Mg-5CCA; and (d) Mg-7.5CCA composites.

3.3. Mechanical Properties

The result of microhardness measurements on Mg and Mg-CCA composites is shown in Table 1. It was observed that the indentation resistance of Mg was significantly increased with the presence of CCA particles. When compared to pure Mg, an increment in hardness of 1.2 times, 1.5 times, and 1.7 times was observed in the Mg-2.5CCA, Mg-5CCA, and Mg-7.5CCA composites, respectively. The localized matrix deformation was constrained by the presence of hard and strong ball-milled CCA particles. The increasing trend of hardness can be due to the addition of an increasing amount of hard CCA reinforcement particles in the Mg matrix.

The compressive properties of pure Mg and Mg composites containing ball-milled CCA particles are listed in Table 2 and Figure 6. When compared to pure Mg, a significant improvement in compressive yield strength of 40%, 57%, and 63% in the Mg-2.5CCA, Mg-5CCA, and Mg-7.5CCA composites was achieved, respectively. In terms of ultimate compressive strength, 57%, 78%, and 79% increments over pure Mg were attained in the Mg-2.5CCA, Mg-5CCA, and Mg-7.5CCA composites, respectively. The results indicated an increasing trend of average compressive strengths with increased addition of ball-milled alloy particles from 2.5 to 7.5 wt % in the Mg matrix. Between the Mg-5CCA and Mg-7.5CCA composites, the strength increment was marginal and the strength level was the same

if the standard deviation is taken into consideration. This can be explained based on the grain size measurement, which shows the occurrence of the same average grain size between the two composite compositions (Table 1). From the compressive failure strain results, the presence of CCA particles had no clear deteriorating effect on the ductility of pure Mg, which showed a similar failure strain to Mg and its composites (Table 2). However, the average failure strain in Mg-5CCA was found to be lower than that in Mg-2.5CCA and Mg-7.5CCA. From the grain size distribution result, a right-skewed distribution was observed with the influence of the small grain size in Mg-5CCA's composition. For materials with coarse grains, a higher compressive strain can be expected due to continuous twinning within the coarse grains. For materials with smaller grains, the compressive strain can be decreased due to less continuity of twinning within the fine grains. This phenomenon was reported in detail in a related paper based on magnesium-based composites [16]. In addition, the ductility increment in this composite can be attributed to the resultant microstructural homogeneity in terms of grain size and particle distribution. The resultant lower failure strain in the Mg-5CCA composite can be accounted for with the influence of small grains from the grain distribution measurement (Figure 4c) and microstructural observation (Figure 5c).

Table 2. Results of room temperature compressive properties.

Materials	0.2% Compressive Yield Strength (MPa)	Ultimate Compressive Strength (MPa)	Compressive Failure Strain (%)
Mg	91 ± 8	263 ± 16	12 ± 2
Mg-2.5 wt % CCA (1.6 vol %)	127 ± 5 (40%)	414 ± 6 (57%)	15 ± 1
Mg-5.0 wt % CCA (3.2 vol %)	143 ± 2 (57%)	469 ± 18 (78%)	10 ± 2
Mg-7.5 wt % CCA (4.9 vol %)	148 ± 4 (63%)	472 ± 19 (79%)	15 ± 2
Mg-6 vol % Ni ₅₀ Ti ₅₀ [17]	89 ± 3	368 ± 8	15.1 ± 1.5
Mg-5 vol % Ni ₆₀ Nb ₄₀ [18]	130 ± 11	320 ± 11	18.4 ± 1.3
AT81-5 vol % SiC [9]	127 ± 10	301 ± 20	11.4 ± 0.5
AZ91D-3 vol % TiC [10]	-	320 *	17 *

* Values approximated from the Compression graph.

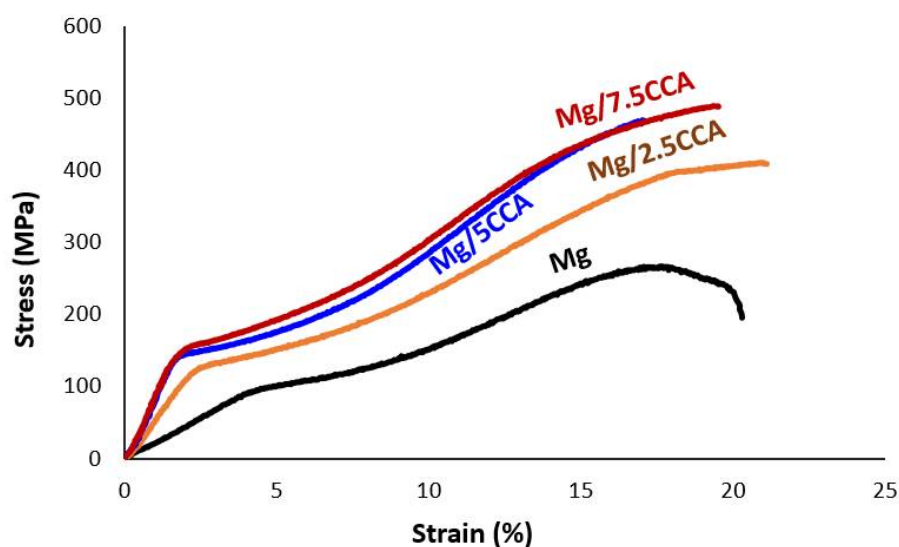


Figure 6. Compressive Stress-Strain curve of the Mg and Mg-CCA composites.

When compared to Mg composites containing ball-milled amorphous particles with a comparable amount of reinforcement addition, a significant improvement in compressive yield strength and ultimate compressive strength was observed in the Mg composite containing CCA particles

while maintaining a similar compressive failure strain level (Table 2). In addition, significantly higher compressive strengths were achieved in the Mg-CCA composites when compared to the Mg-alloy-based composites containing micron size particles. This indicates the beneficial effect of CCA alloy particles for property enhancement in the composites under compressive loading. Furthermore, it shows the suitability and compatibility of this new type of CCA alloy particle as a reinforcement in an Mg matrix.

Fracture surface studies were done on Mg and its composites and the representative fractographs are shown in Figure 7. From the fractographs, the appearance of smooth fracture surfaces can be seen in the Mg, Mg-2.5CCA, and Mg-7.5CCA composites. In case of the Mg-5CCA composite, the appearance of ragged and rough fracture features was observed. The observed fracture features conform with the resultant compressive failure strain values presented in Table 2, indicating the reduced ductility attained in the Mg-5CCA composite's composition when compared to the Mg, Mg-2.5CCA, and Mg-7.5CCA composites (Figure 6).

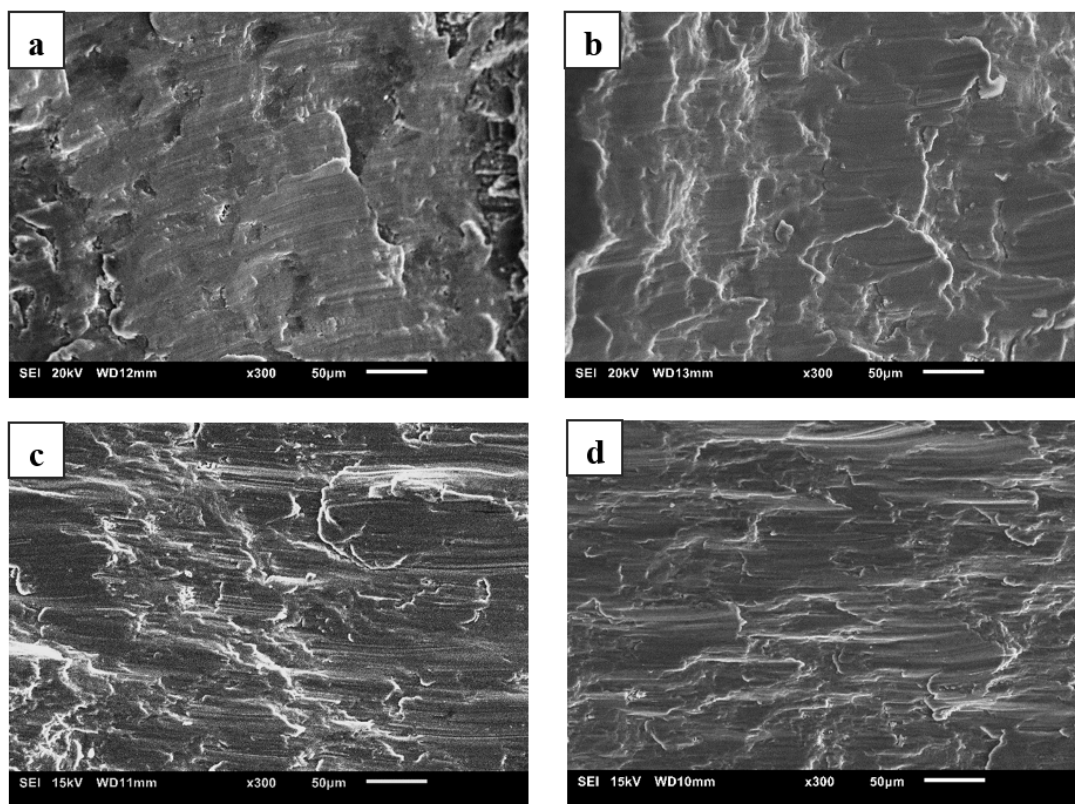


Figure 7. Representative fractographs of: (a) Mg; and the (b) Mg-2.5CCA; (c) Mg-5CCA; and (d) Mg-7.5CCA composites.

4. Conclusions

Based on the interrelation between the microstructural evolution and mechanical properties of the Mg-CCA composites developed in this work, conclusions are drawn as follows:

1. New Mg-CCA composites can be successfully developed using a powder metallurgy route incorporating microwave sintering and hot extrusion.
2. The addition of ball-milled CCA reinforcement particles assisted in a significant refinement of the matrix grain size. The measurement on the grain size distribution showed a normal distribution in the Mg, Mg-2.5CCA, and Mg-7.5CCA composite compositions while a right-skewed distribution was observed in the Mg-5CCA composite.

3. Hardness increased with an increasing amount of reinforcement addition in the Mg-CCA composites. The maximum microhardness of 80 HV was achieved in the Mg-7.5 wt % CCA composite.
4. The compressive yield strength and ultimate compressive strength were significantly enhanced in the Mg-CCA composites while maintaining the same ductility levels as unreinforced Mg. The newly developed Mg-CCA composites showed higher strength under compressive loading when compared to Mg composites containing ball-milled amorphous particles and Mg-alloy-based composites containing micron-size particle reinforcement. The achievement of enhanced mechanical properties in Mg-CCA composites highlighted the effectiveness of using ball-milled CCA particles as a reinforcement in Mg.

Acknowledgments: The authors would like to acknowledge the Ministry of Education Academic Research Funding (WBS# R-265-000-586-114) for the financial support in carrying out this research work.

Author Contributions: Manoj Gupta and Khin Sandar Tun proposed the original project and supervised the investigation. Yuming Zhang, Gururaj Parande, and Vyasraj Manakari performed processing. Khin Sandar Tun, Yuming Zhang, Gururaj Parande, and Vyasraj Manakari performed testing and characterization. Khin Sandar Tun performed data analysis and wrote the paper. Manoj Gupta contributed consultation, data analysis, and paper review.

Conflicts of Interest: The authors declare no conflict of interest.

References

1. Kulekci, M.K. Magnesium and its alloys applications in automotive industry. *Int. J. Adv. Manuf. Technol.* **2008**, *39*, 851–865. [CrossRef]
2. Caton, P.D. Magnesium—An old material with new applications. *Mater. Des.* **1991**, *12*, 309–316. [CrossRef]
3. International Magnesium Association. Available online: http://c.ymcdn.com/sites/intlmag.site-ym.com/resource/resmgr/docs/automotive/MgShowcase15_Feb2011.pdf (accessed on 28 January 2018).
4. Kainer, K.U.; Buch, F. The Current State of Technology and Potential for further Development of Magnesium Applications. In *Magnesium Alloys and Technology*; Wiley-VCH: Weinheim, Germany, 2003; pp. 1–22.
5. Housh, S.; Mikucki, B.; Stevenson, A. Selection and Application of Magnesium and Magnesium Alloys. In *ASM Handbook*, 10th ed.; ASM International: Materials Park, OH, USA, 1990; Volume 2, pp. 455–479.
6. Rohatgi, P.K. Metal Matrix Composites. *Def. Sci. J.* **1993**, *43*, 323–349. [CrossRef]
7. Lloyd, D.J. Particle reinforced aluminum and magnesium matrix composites. *Int. Mater. Rev.* **1994**, *39*, 1–23. [CrossRef]
8. Tjong, S.C. Novel nanoparticle reinforced metal matrix composites with enhanced mechanical properties. *Adv. Eng. Mater.* **2007**, *9*, 639–652. [CrossRef]
9. Luo, D.; Pei, C.-H.; Rong, J.; Wang, H.-Y.; Li, Q.; Jiang, Q.-C. Microstructure and mechanical properties of SiC particles reinforced Mg–8Al–1Sn magnesium matrix composites fabricated by powder metallurgy. *Powder Metall.* **2015**, *58*, 349–353. [CrossRef]
10. Cao, W.; Zhang, C.; Fan, T.; Zhang, D. In Situ Synthesis and Compressive Deformation Behaviors of TiC Reinforced Magnesium Matrix Composites. *Mater. Trans.* **2008**, *49*, 2686–2691. [CrossRef]
11. Gupta, M.; Nai, S.M.L. *Magnesium, Magnesium Alloys and Magnesium Composites*, 1st ed.; John Wiley & Sons: Hoboken, NJ, USA, 2011; pp. 113–205. ISBN 978-0-47-049417-2.
12. Perez, P.; Garces, G.; Adeva, P. Mechanical properties of a Mg–10 (vol %)Ti composite. *Comp. Sci. Technol.* **2004**, *64*, 145–151. [CrossRef]
13. Tun, K.S.; Gupta, M.; Srivatsan, T.S. Investigating influence of hybrid (yttria + copper) nanoparticulate reinforcements on microstructural development and tensile response of magnesium. *Mater. Sci. Technol.* **2010**, *26*, 87–94. [CrossRef]
14. Tun, K.S.; Gupta, M. Development of magnesium (yttria + nickel) hybrid nanocomposites using hybrid microwave sintering: Microstructure and tensile properties. *J. Alloy. Compd.* **2009**, *487*, 76–82. [CrossRef]
15. Tun, K.S.; Gupta, M. Role of microstructure and texture on compressive strength improvement of Mg/(Y₂O₃ + Cu) hybrid nanocomposites. *J. Comp. Mater.* **2010**, *44*, 3033–3050. [CrossRef]

16. Tun, K.S.; Gupta, M. Compressive deformation behavior of Mg and Mg/(Y₂O₃ + Ni) nanocomposite. *Mater. Sci. Eng. A* **2010**, *527*, 5550–5556. [[CrossRef](#)]
17. Sankaranarayanan, S.; Hemanth Shankar, V.; Jayalakshmi, S.; Nguyen, Q.B.; Gupta, M. Development of high performance magnesium composites using Ni₅₀Ti₅₀ metallic glass reinforcement and microwave sintering approach. *J. Alloy. Compd.* **2015**, *627*, 192–199. [[CrossRef](#)]
18. Jayalakshmi, S.; Sahu, S.; Sankaranarayanan, S.; Gupta, S.; Gupta, M. Development of novel Mg–Ni₆₀Nb₄₀ amorphous particle reinforced composites with enhanced hardness and compressive response. *Mater. Des.* **2014**, *53*, 849–855. [[CrossRef](#)]
19. Jayalakshmi, S.; Gupta, M. *Metallic Amorphous Alloy Reinforcements in Light Metal Matrices*, 1st ed.; Springer: Cham, Switzerland, 2015; pp. 85–105. ISBN 978-3-319-15015-4.
20. Tun, K.S.; Srivatsan, T.S.; Kumar, A.; Gupta, M. Synthesis of Light Weight High Entropy Alloys: Characterization of Microstructure and Mechanical Response. In Proceedings of the Twenty-Sixth International Conference on the Processing and Fabrication of the Advanced Materials (PFAM XXVI), Jeonju, Korea, 16–21 October 2017.
21. Inem, B. Dynamic recrystallization in a thermomechanically processed metal matrix composite. *Mater. Sci. Eng. A* **1995**, *197*, 91–95. [[CrossRef](#)]
22. Wang, X.J.; Wu, K.; Zhang, H.F.; Huang, W.H.; Chang, H.; Gan, W.M.; Zheng, M.Y.; Peng, D.L. Effect of hot extrusion on the microstructure of a particulate reinforced magnesium matrix composite. *Mater. Sci. Eng. A* **2007**, *465*, 78–84. [[CrossRef](#)]
23. Chan, H.M.; Humphreys, F.J. The recrystallisation of aluminium-silicon alloys containing a bimodal particle distribution. *Acta Metall.* **1984**, *32*, 235–243. [[CrossRef](#)]



© 2018 by the authors. Licensee MDPI, Basel, Switzerland. This article is an open access article distributed under the terms and conditions of the Creative Commons Attribution (CC BY) license (<http://creativecommons.org/licenses/by/4.0/>).